Phase of the Riemann ζ function and the inverted harmonic oscillator

R.K. Bhaduri, Avinash Khare,* and J. Law,†
Department of Physics and Astronomy, McMaster University, Hamilton, Ontario, Canada L8S 4M1
(Received 2 December 1994)

The Argand diagram is used to display some characteristics of the Riemann ζ function. The zeros of the ζ function on the complex plane give rise to an infinite sequence of closed loops, all passing through the origin of the diagram. The behavior of the phase of the ζ function on and off the line of zeros is studied. Up to some distance from the line of the complex zeros, the phase angle is shown to still retain their memory. The Argand plots also lead to an analogy with the scattering amplitude and an approximate rule for the location of the zeros. The smooth phase of the ζ function along the line of the zeros is related to the quantum density of states of an inverted oscillator.

PACS number(s): 05.45.+b, 03.65.Nk, 02.90.+p

I. INTRODUCTION

The Riemann zeta function $\zeta(s)$ of the complex variable $s = \sigma + it$, defined by the equation (for $\sigma > 0$)

$$\zeta(s) = \sum_{n=1}^{\infty} \frac{1}{n^s}, \tag{1}$$

has an infinite number of zeros on the half-line $\sigma = \frac{1}{2}$ [1]. These zeros are of great interest to mathematicians from the number theoretic point of view [2,3], and to physicists interested in quantum chaos and the periodic orbit theory [4–6]. Along this line, as a function of t, every time $\zeta(s)$ changes sign, a discontinuous jump by π in the phase angle is introduced. Otherwise the phase angle is a smooth function of t. The smooth part of the phase angle itself is very interesting, since it counts the number of zeros on the 1/2 line fairly accurately. In this paper we bring out some of the interesting properties of $\zeta(s)$ by displaying it on an Argand diagram, where Re$\zeta(s)$ (along the x axis), is plotted against Im $\zeta(s)$ (y axis). For $\sigma = 1/2$, the plot yields an infinite sequence of closed loops, one for every zero of the ζ function, all going through the origin. We show that as one moves somewhat away from the $\sigma = 1/2$ line, the phase angle still has sharp drops at those values of t which have zeros on the 1/2 axis. However, this "memory" of the zeros begins to fade as one moves along the real axis. We also point out the similarity in the Argand diagrams for $\zeta(1/2 + it)$ and the resonant quantum scattering amplitude, and this analogy, although flawed, leads directly to an approximate quantization condition for the location of the zeros [7,8]. We demonstrate that for $\sigma = 1/2$, the smooth part of the phase angle of $\zeta(s)$ is closely related to the phase shift of an inverted half harmonic oscillator.

II. THE PHASE ANGLE AND THE ARGAND DIAGRAM

We start by giving some standard results for the Riemann zeta function $\zeta(s)$. Using the fundamental functional relationship between $\zeta(s)$ and $\zeta(1-s)$, it is easy to show that [2]

$$\zeta(\tfrac{1}{2} - it) = (\pi)^{-it} \frac{\Gamma(\frac{1}{4} + \frac{it}{2})}{\Gamma(\frac{1}{4} - \frac{it}{2})} \zeta(\tfrac{1}{2} + it), \tag{2}$$

where $\Gamma(z)$ denotes the γ function of the argument z. We may further write

$$\zeta(\tfrac{1}{2} + it) = Z(t) \exp[-i\theta(t)], \tag{3}$$

where $Z(t)$ is real and $\theta(t)$ is the phase angle, with the convention that $\theta(0) = \pi$. Using Eqs. (1) and (2) it follows that

$$\exp[2i\theta(t)] = \exp(-it \ln \pi) \frac{\Gamma(\frac{1}{4} + \frac{it}{2})}{\Gamma(\frac{1}{4} - \frac{it}{2})}. \tag{4}$$

The phase θ, as defined above, is smooth in the sense that it does not include the jumps by π due to the zeros of $Z(t)$. Nevertheless, the number of zeros between 0 and t on the $\sigma = 1/2$ line is counted fairly accurately by $\theta(t)$, as will become clear from the Argand diagram. Note that

$$\frac{\theta(t)}{\pi} = -\frac{t}{2\pi} \ln \pi + \frac{1}{2\pi} \mathrm{Im} \left[\ln \Gamma \left(\frac{1}{4} + \frac{it}{2} \right) - \ln \Gamma \left(\frac{1}{4} - \frac{it}{2} \right) \right] + 1, \tag{5}$$

which satisfies the condition that $\theta(0) = \pi$. The density of zeros is given by

*Also at: Institute of Physics, Sachivalaya Marg, Bhubaneswar-751 005, India.

†Physics Department, University of Guelph, Guelph, Ontario, Canada, NIG 2W1.

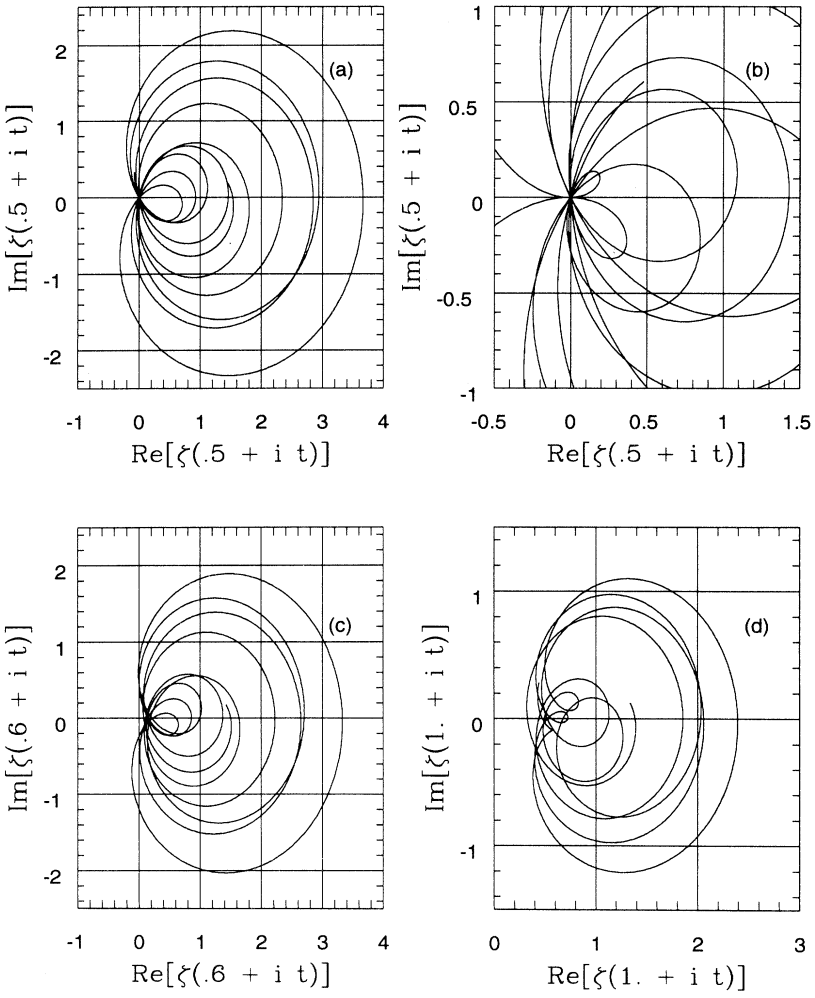

FIG. 1. The Argand diagrams for $\zeta(\sigma+it)$ for increasing t and fixed σ. (a) $\zeta(1/2+it)$ in the range $t = 9 - 50$. The lower limit for t is chosen so as not to miss the Gram point flanking the lowest zero at $t = 14.13$. (b) $\zeta(1/2+it)$ for $t = 280 - 300$, showing the two loops without the corresponding Gram points. (c) $\zeta(0.6+it)$ for $t = 9 - 50$ to show the defocusing at the origin. (d) $\zeta(1+it)$ for $t = 9 - 50$. Note the pronounced shift of the diagram away from the origin in this case.

$$\frac{1}{\pi}\frac{d\theta}{dt} = \frac{1}{2\pi}\left\{-\ln\pi + \mathrm{Re}\left[\Psi\left(\frac{1}{4}+i\frac{t}{2}\right)\right]\right\}, \qquad (6)$$

where the digamma function is defined as $\Psi(z) = \Gamma'(z)/\Gamma(z)$. From the above, the asymptotic expression for $\theta(t)$ may be obtained immediately by making asymptotic expansion of the Γ functions. We denote this by $\tilde{\theta}(t)$ and it is given by

$$\frac{1}{\pi}\tilde{\theta}(t) = \left(\frac{t}{2\pi}\right)\ln\left(\frac{t}{2\pi}\right) - \left(\frac{t}{2\pi}\right) + \frac{7}{8} + \frac{1}{48\pi t} + \cdots . \qquad (7)$$

To bring out some characteristics of the function $\zeta(1/2+it)$, we plot its Argand diagram in Fig. 1(a) in the range $t = 9$ to $t = 50$. This shows a sequence of closed loops, one for every zero of the ζ function. At a zero of $\zeta(1/2+it)$, both its real and imaginary parts are zero at the same value of t, and therefore every loop converges at the origin. The intercepts on the real axis are the so-called "Gram points," where only the imaginary part of $\zeta(s)$ is zero, due to the phase angle $\theta(t) = n\pi$. With infrequent exceptions, there is one Gram point between two consecutive zeros of the ζ function. The first two exceptions to this rule occur for the 126th and the 134th zeros at $t = 282.455$ and 295.584, respectively [2]. The Argand diagram in Fig. 1(b) clearly shows that for these cases, the loop structure still persists, even though the Gram points are missing. In Figs. 1(c) and 1(d) Argand diagrams are drawn away from the 1/2 axis, for $\sigma = 0.6$ and $\sigma = 1$, respectively. These clearly show the defocusing at the origin due to the absence of the zeros in the ζ function. Moreover, the number of intercepts along the real axis in the Argand diagrams now show a large increase compared to the $\sigma = 1/2$ case, whereas the intercepts on the imaginary axis are few or nonexistent. This is a reflection of the change in the behavior of the phase $\theta(t)$ away from the $\sigma = 1/2$ line. In Fig. 2(a), the phase angle $\theta(t)$, as determined by Eq. (5), is plotted as a function of t on the 1/2 axis. This phase angle is a smooth function of t because the jumps by π at every

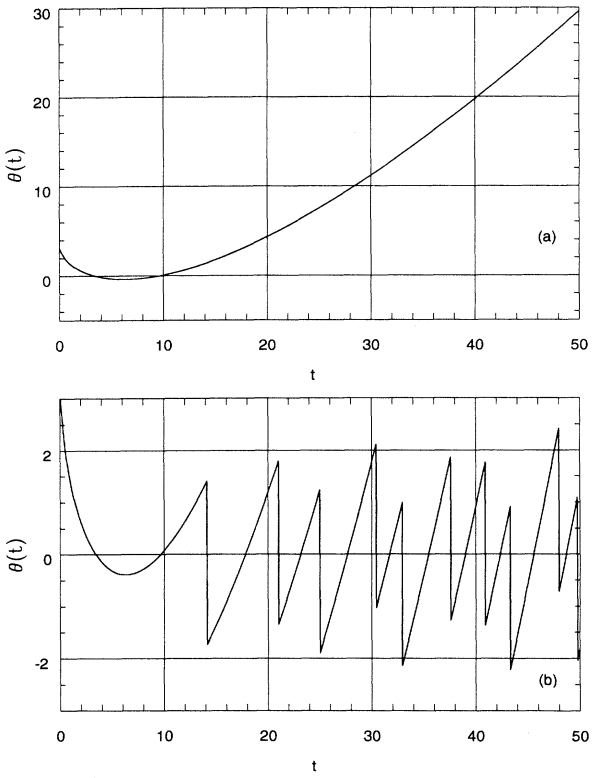

FIG. 2. (a) The smooth phase angle of $\zeta(1/2+it)$, as defined by Eq. (5), is plotted as a function of $t = 0 - 50$. (b) The discontinuities of π in the phase angle $\theta(t)$ at $\sigma = 0.5$ at the position of the zeros are shown. The total phase is given by the superposition of (b) on (a).

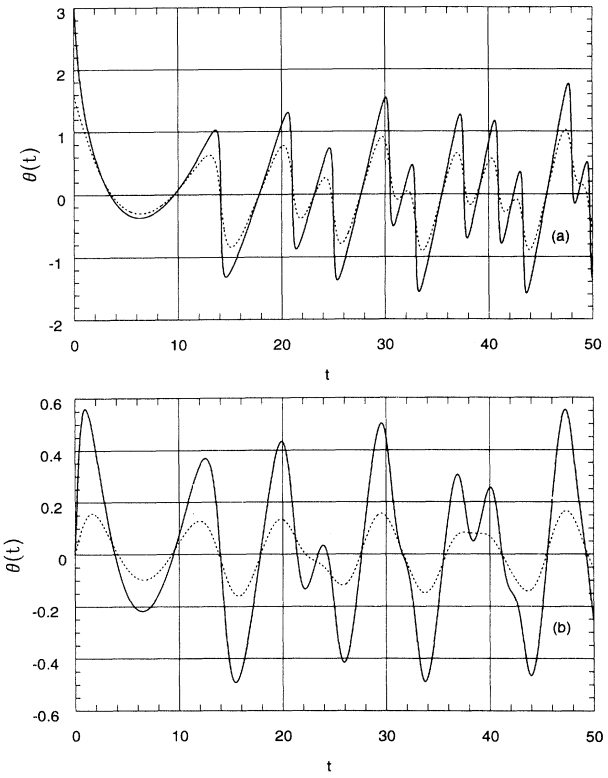

FIG. 3. The exact phase angle of $\zeta(\sigma+it)$ is plotted as a function of $t = 0 - 50$ for (a) $\sigma = 0.6$ (solid line) and $\sigma = 1.0$ (dotted line). (b) The same as above, for $\sigma = 1.6$ (solid line) and $\sigma = 3.0$ (dotted line). Note that the vertical scale is expanded in (b).

zero (due to the change in the sign of the ζ function) is not registered by it. These discontinuities are shown separately in Fig. 2(b). The smooth phase keeps increasing monotonically with t, since the curve in the complex plane passes through the origin at every zero . The behavior of the phase angle $\theta(t)$ away from the 1/2 axis is shown in Fig. 3. Note that for $\sigma \neq 1/2$, $\zeta(s)$ and $\zeta(1-s)$ are not complex conjugate of each other. Therefore Eq. (4) no longer holds in such a situation. There is no monotonic increase in the phase angle now, although the zigzag character of $\theta(t)$ reflects that some memory of the zeros is still retained. Indeed, Fig. 3(a) shows that the phases at $s = 0.6 + it$ (solid curve) and $s = 1.0 + it$ (dotted curve) as a function of t drop precipitously precisely at those values of t for which there is a zero on the 1/2 axis. These drops, though still there, are not so pronounced for $s = 1.6+it$, and are smoothed out for $s = 3+it$ [solid and dotted curves, respectively, Fig. 3(b)]. Nevertheless, the "chaotic" characteristic of the phase angle off the 1/2 axis is still due to the zeros on the 1/2 axis. This is apparent in Fig. 4, where the derivative $d\theta/dt$ is plotted as a function of t for $\sigma = 0.6, 1$ [Fig. 4(a)] and $\sigma = 1.6, 3.0$ [Fig. 4(b)]. Whereas the position of all the ten zeros of $\zeta(s)$ in the range $t = 0 - 50$ may be read off from the curves for $\sigma = 0.6$, 1, and 1.6, the undulations of the slope are gentler for $\sigma = 3$, with concomitant loss of information. Note that there is a spurious dip near $t = 0$ in all the curves in Fig. 4. It must be mentioned that the phase angle for $s = 1 + it$ is well studied in relation to the quantum scattering phase shift of a particle on a surface of constant negative curvature [9–11].

Finally, in Figs. 5(a) and 5(b), the Argand diagrams of the ζ function are drawn for a much larger range of t, from 1 to 500, on and off the 1/2 axis. Note that the scale for $\sigma = 1$ is expanded compared to that for $\sigma = 1/2$. Borrowing from the terminology of the motion of a particle in phase space, it is as if there is an "attractor" at the origin for $\sigma = 1/2$ [Fig. 5(a)], which is absent from the more disorderly tracks of Fig. 5(b), which is drawn along the $\sigma = 1$ line. The latter figure also shows that the real part of the ζ function is always positive for $\sigma = 1$ for this entire range of t.

III. ANALOGY WITH THE SCATTERING AMPLITUDE

The loop structure of the ζ function at $\sigma = 1/2$, with some near-circular shapes, is reminiscent of the Argand plots for the scattering amplitudes of different partial

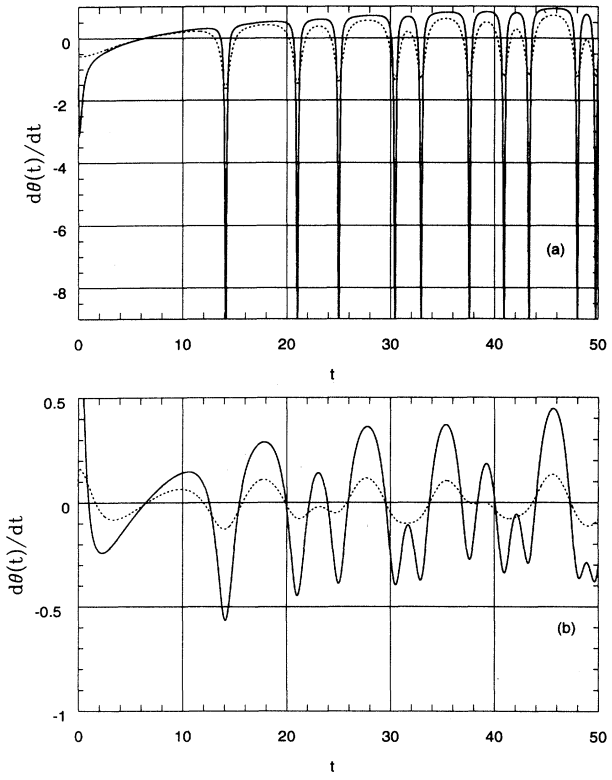

FIG. 4. The derivative of the phase angle of $\zeta(\sigma + it)$ from Fig. 3 is plotted as a function of $t = 0 - 50$ for (a) $\sigma = 0.6$ (solid curve) and $\sigma = 1.0$ (dotted curve); (b) $\sigma = 1.6$ (solid curve) and $\sigma = 3.0$ (dotted curve). The verical scale in (b) is again expanded for clarity.

waves in the analysis of resonances, for example, in pion-nucleon scattering [12]. Consider the partial wave amplitude $f_l(k)$, defined in terms of the partial wave phase-shift $\delta_l(k)$ and the inelasticity parameter $\eta_l(k)$,

$$f_l(k) = [\eta_l \exp(2i\delta_l) - 1]/2ik. \tag{8}$$

Here l refers to the angular momentum and k the wave number. Note that $\mathrm{Im}\, f_l(k)$ is never negative, since the inelasticity parameter η_l is always less than one. One generally plots an Argand diagram with $2k\,\mathrm{Im}\, f_l(k)$ along the x axis for various values of k. For the case of no inelasticity ($\eta_l = 1$) and a single resonance, the Argand diagram is a perfect circle with unit radius, with the center on the imaginary axis at 1. By comparing this with Fig. 1(a) at $\sigma = 1/2$ we see that the real and the imaginary parts are interchanged in the latter, but otherwise there is a strong similarity, with many of the loops having inelasticity. This analogy is flawed, however, since $\mathrm{Re}\zeta(1/2 + it)$ does become negative in small islands of t. Nevertheless, if these islands are ignored, then the phase shift δ_l may be identified with the phase angle $\theta + \pi/2$, with each closed loop in Fig. 1(a) being regarded as in isolated resonance. In this approximation, the Gram points occur as before for $\sin\theta = 0$, while the zeros of

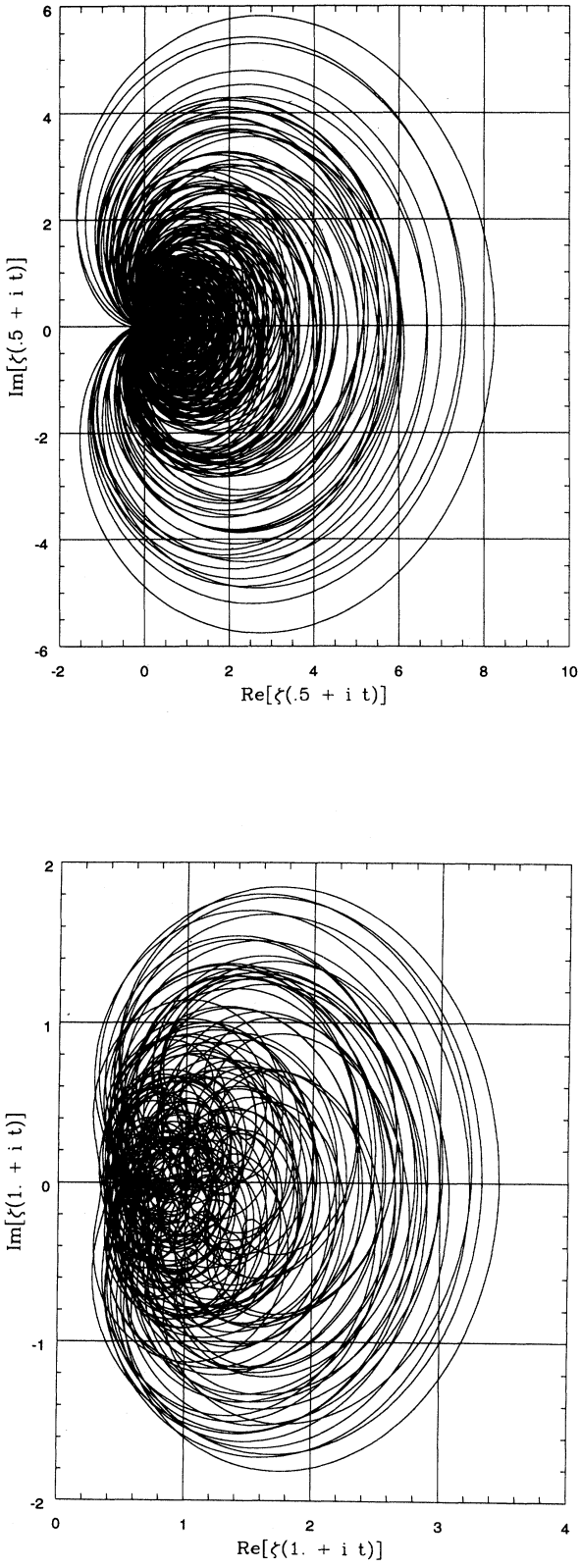

FIG. 5. The Argand diagrams of the Riemann ζ function for the wider range of t values, from $t = 9-500$. (a) $\zeta(1/2+it)$, and (b) $\zeta(1 + it)$.

$\zeta(1/2+it)$ are given by the condition

$$\cos\theta = 0, \quad \theta = (m+1/2)\pi, \quad m = 1,2,\ldots . \tag{9}$$

This condition for the location of the zeros was also obtained by Berry [7] from the first term in his approximate formula. Equation (8) has roots that yield the zeros on the 1/2 axis with an error of at most 3%.

IV. THE INVERTED HARMONIC OSCILLATOR

As mentioned earlier, for $\sigma = 1$, the phase $\theta(t)$ is intimately connected to the quantum scattering of a particle on a saddlelike surface. On the $\sigma = 1/2$ line, our analogy with the scattering amplitude also suggests that the phase angle $\theta(t)$ is related to a scattering phase shift. We now demonstrate that the scattering of a nonrelativistic particle by an inverted harmonic oscillator with a hard wall at the origin generates a phase shift that is closely related to $\theta(t)$. Indeed, we show that the quantum density of states for this problem is essentially the same as Eq. (5) for the density of the zeros. Consider the Schrödinger equation for $x \geq 0$,

$$-\frac{\hbar^2}{2m}\frac{d^2}{dx^2}\Phi - \frac{1}{2}m\omega^2 x^2 \Phi = E\Phi, \tag{10}$$

and impose the boundary condition that the wave function Φ vanishes at the origin. Putting $x^2 = y$, $\Phi = y^{-\frac{1}{4}}\phi$, it becomes

$$\frac{d^2}{dy^2}\phi - \frac{l(l+1)}{y^2}\phi - \frac{kt}{y}\phi + k^2\phi = 0. \tag{11}$$

In the above equation,

$$l = -\frac{1}{4}, \quad k = \frac{m\omega}{2\hbar}, \quad t = -\frac{E}{\hbar\omega}. \tag{12}$$

This is effectively a three-dimensional Schrödinger equation for a repulsive Coulomb potential in the variable y. To obtain the phase shift, we write the asymptotic solution of the above equation [13] as

$$\phi(y) \sim \sin\left(ky - \frac{t}{2}\ln(2ky) - \frac{l\pi}{2} + \eta_l\right), \tag{13}$$

where η_l is the phase shift with respect to the distorted Coulomb wave, given by $\arg\Gamma(l+1+it/2)$. For our one-dimensional problem, only $l = -1/4$ is relevant. For this case, omitting the subscript l, the phase shift η is

$$\eta = \arg\Gamma\left(\frac{3}{4} + \frac{it}{2}\right). \tag{14}$$

Using the identity [14]

$$\Gamma(\tfrac{1}{4}+iy)\,\Gamma(\tfrac{3}{4}-iy) = \frac{\pi\sqrt{2}}{\cosh\pi y + i\sinh\pi y}. \tag{15}$$

The number of quantum states $n(t)$, between 0 and t, is then given by

$$n(t) = \frac{\eta(t)}{\pi} = \frac{C}{2\pi} + \frac{1}{2\pi}\mathrm{Im}\left[\ln\Gamma\left(\frac{1}{4}+i\frac{t}{2}\right) - \ln\Gamma\left(\frac{1}{4}-i\frac{t}{2}\right)\right]. \tag{16}$$

In the above equation, C is a smooth function given by

$$C = \frac{\pi}{2} - \tan^{-1}(\mathrm{cosech}\pi t\,). \tag{17}$$

Note from above that the expression for $\eta(t)$ is not quite identical to $\theta(t)$ as defined in Eq. (5). However, their derivatives, the quantum density of states, only differ by a constant and an exponentially small term. It should also be pointed out that even if we had started with a full inverted harmonic oscillator (rather than the half-oscillator), the same conclusion would be reached, even though there may arise some nonuniqueness in the choice of the boundary condition. The inverted harmonic oscillator problem was studied by a number of authors in the past [15,16] in relation to time-delay, and by others [17–20] in connection to string theory. No connection, however, was made to the phase of $\zeta(1/2+it)$.

V. SUMMARY

In summary, we recapitulate the main points made in this paper. Traditionally, the behavior of the zeros of the Riemann ζ function on the 1/2 axis is associated with the bound state problem of a quantum Hamiltonian. We, on the other hand, focus on the scattering problem. We use the Argand diagram construction for the Riemann ζ function to visualize how the smooth phase $\theta(t)$ acts as a counter for the zeros of $Z(t)$. Off the 1/2 axis, the zigzag pattern of the phase shift as a function of t transforms to smooth undulations which still retain the memory of the zeros. This memory fades, however, as the distance from the 1/2 axis increases. We also note from the Argand diagrams of the ζ function its analogy with the scattering amplitude, and the approximate condition [Eq. (9)] for the location of the zeros. The smooth part of the phase angle of the ζ function on the $\sigma = 1/2$ line is related to the quantum phase shift of a potential. It is perhaps not surprising that this potential that generates the smooth phase is as simple as the inverted harmonic oscillator. The chaotic jumps in the phase, shown in Fig. 2(b), have been left out from this. It is known that for the chaotic phase at $\sigma = 1$ [9–11], the motion of the particle is on the surface of a saddle. The orbits in this case are all unstable. It is as if the smooth phase on the 1/2 line still remembered a section of the saddle, i.e., the inverted oscillator. Finally, we suggest that the Argand

diagram construction may also be useful for the Selberg ζ function, and shed light on the quantization condition for quantum chaos [8]. This last point is under current investigation.

One of the authors (A.K.) would like to acknowledge the hospitality of the physics department of McMaster University. This research was supported by Grants from NSERC of Canada.

---

[1] G.H. Hardy, Comptes Rendus **CLVIII**, 280 (1914).
[2] H.M. Edwards, *Riemann's Zeta Function* (Academic, New York, 1974).
[3] A. Ivic, *The Riemann Zeta Function* (Wiley, New York, 1985).
[4] M.V. Berry, Proc. R. Soc. London Ser. A **400**, 229 (1985).
[5] M.C. Gutzwiller, *Chaos in Classical and Quantum Mechanics* (Springer Verlag, New York, 1991).
[6] Hua Wu and D.W.L. Sprung, Phys. Rev. E **48**, 2595 (1993).
[7] M.V. Berry, in *Quantum Chaos and Statistical Nuclear Physics*, edited by T.H. Seligman and H. Nishioka, Lecture Notes in Physics, Vol. 263 (Springer Verlag, New York, 1986), p. 1.
[8] R. Aurich and F. Steiner, Phys. Rev. A **45**, 583 (1992).
[9] B.S. Pavlov and L.D. Faddeev, Sov. Math. **3**, 522 (1975).
[10] P. Lax and R.S. Philips, *Scattering Theory for Automorphic Functions* (Princeton University Press, Princeton, NJ, 1976).
[11] M.C. Gutzwiller, Physica D **7**, 341 (1983).
[12] R.K. Bhaduri, *Models of the Nucleon* (Addison Wesley, Reading, MA, 1988), p. 27.
[13] S. Flügge, *Practical Quantum Mechanics* (Springer Verlag, New York, 1974), p. 293.
[14] *Handbook of Mathematical Functions*, edited by M. Abramowitz and I.A. Stegun (Dover, New York, 1965), p. 256.
[15] K.W. Ford, D.L. Hill, M. Wakano, and J.A. Wheeler, Ann. Phys. (N.Y.) **7**, 239 (1959).
[16] G. Barton, Ann. Phys. (N.Y.) **166**, 322 (1986).
[17] E. Brézin, V.A. Kazakov, and Al.B. Zamolodchikov, Nucl. Phys. **B338**, 673 (1990).
[18] D.J. Gross and N. Miljković, Phys. Lett. B **238**, 217 (1990).
[19] G. Parisi, Phys. Lett. B **238**, 213 (1990).
[20] P. Ginsparg and J. Zinn-Justin, Phys. Lett. B **240**, 333 (1990).